The Deuteron Magnetic Resonance of Tin(II) Chloride Dihydrate Single Crystals in High- and Low-temperature Phases

Hideko KIRIYAMA* and Osamu NAKAMURA**

Department of Chemistry, Faculty of Science, Kobe University, Nada-ku, Kobe 657

***Government Industrial Research Institute, Osaka, Midorigaoka 1, Ikeda, Osaka 563*

(Received September 3, 1979)

The deuteron magnetic resonance spectra of $SnCl_2 \cdot 2D_2O$ single crystals have been measured from 208 to 300 K in order to elucidate the static and dynamic structures of water molecules in connection with the phase transition occuring at 234 K. The deuteron quadrupole coupling constants (asymmetry parameters) were determined at 208 K for four non-equivalent water deuterons. These values are 194.2±0.3 (0.066±0.004), 193.2±0.5 (0.112±0.003), 223.3±0.4 (0.206±0.003), and 244.0±0.4 kHz (0.058±0.003), depending largely on the hydrogen-bond strength or the D···O distance. The deuteron arrangements deduced from the EFG tensors agreed well with the ordered structure reported by an earlier ND study. The dynamical process of deuterons responsible for the high-temperature disordered structure was analyzed with the aid of the ND results and was ascribed to a combination of the flip motion of water molecules about each two-fold axis and their rotational motion around each pseudo-three-fold axis.

The phase transition in $SnCl_2 \cdot 2H_2O$ (abbreviated as SCD) was first found at 218 K (at 234 K for its deuterium analogue) from an anomaly in the dielectric constant measured by Kiriyama and Kiriyama.[1] An earlier X-ray work showed that two kinds of water molecules are arranged alternately to form a characteristic H-bonded layer in the crystal lattice, and also that the phase transition is accompanied by no distinct change in the structure of non-hydrogen atoms.[2] A subsequent neutron diffraction (ND) experiment determined the ordered and disordered arrangements of deuterons below and above the phase-transition temperature, T_t, respectively.[3,4] On the other hand, proton (PMR) and deuteron (DMR) magnetic resonance studies provided direct evidence that the phase transition is due to the ordering of hydrogen (or deuterium) atoms in the H-bonded network.[5] A closer X-ray examination of the structure has disclosed that, in the vicinity of T_t, the [100] and [001] axial lengths and, consequently, the three H-bonded O···O distances steeply change in association with the ordering of the hydrogen atoms.[4]

The ordering process of water hydrogens and the various critical phenomena upon the phase transition were investigated in detail by means of heat-capacity[6] and dielectric measurements[7] as well as by Raman spectroscopies.[8,9] A statistical theory developed for use with the two-dimensional H-bonded network by Salinas and Nagle is helpful in understanding the mechanism of the phase transition as well.[10]

In order to locate the hydrogen atoms in the low-temperature phase and to clarify their dynamic nature, involving the motion of the water molecules in the high-temperature phase, DMR and PMR experiments were carried out using single crystals. Some of these results have been reported previously.[1,5,11]

Experimental

Sample. A commercially available extra-pure reagent, SCD, was ground into a fine powder and then dehydrated in a vacuum desiccator for 12 d at room temperature. The anhydrous sample so obtained was identified by means of its X-ray powder patterns and IR spectra. For the present DMR work, large single crystals were needed to obtain suitable signals. About $20 \times 15 \times 40$ mm^3 in size, they were grown by very slow cooling from saturated aqueous (D_2O) solution of the anhydrate, $SnCl_2$, which had been acidified with DCl. The crystal shape was an elongated prism parallel to the [001] axis, with well-developed side planes, (100) and (110). All the interfacial angles of a deuterated crystal were identical to those of the non-deuterated one, within the limits of experimental error, in accord with the fact that the lattice constants of the two compounds are almost the same.[4] The single crystals were cut and shaped into cylindrical rods, typically 15 mm in diameter × 20 mm long. The axes of the three cylinders were chosen to be parallel to the crystallographic b and c axes, and the normal, to the (100) plane; the last direction will, hereinafter, be referred to as a* axis for convenience.

Measurements. The deuteron magnetic resonance spectra were measured at the Larmor frequency of 6.9 MHz with a frequency-variable, Pound-Watkins-type spectrometer and at 8 MHz with a bridge-type spectrometer (JNM-8, JEOL). The quadrupole effect on NMR or quadrupole splitting was measured at five-degree intervals of rotation angle about each of the mutually perpendicular axes, a*, b, and c. The temperature of a sample was measured by the use of a calibrated copper-constantan thermocouple and was controlled to ±0.3 K throughout the experiments.

Preliminary Remarks

Crystal Structure. The previous X-ray examination showed that no significant isotope effects on the lattice parameter and on the crystal structure are observed on deuterium substitution. Therefore, unless otherwise noted, the description of the structure will be concerned with ordinary $SnCl_2 \cdot 2H_2O$. The crystal is monoclinic, with the space group $P2_1/c$ and with $Z=4$. The lattice parameters are $a=9.158$, $b=7.156$, $c=8.942$ Å, and $\beta=114.50°$ at 88 K, and $a=9.320$, $b=7.277$, $c=8.970$ Å, and $\beta=114.91°$ at 293 K.[2,4] The unit cell contains two kinds of water molecules; the first, $H_2O(1)$, coordinates to a tin(II) atom to form a trigonal pyramid of the dichloroaquatin(II) complex, $SnCl_2 \cdot OH_2$, whereas the second, $H_2O(2)$, does not (Fig. 1). These two kinds of water molecules are alternately connected by three O–H···O-type H-bonds, and the resulting sheets run parallel to the (100) plane. On the assumption of a double-minimum

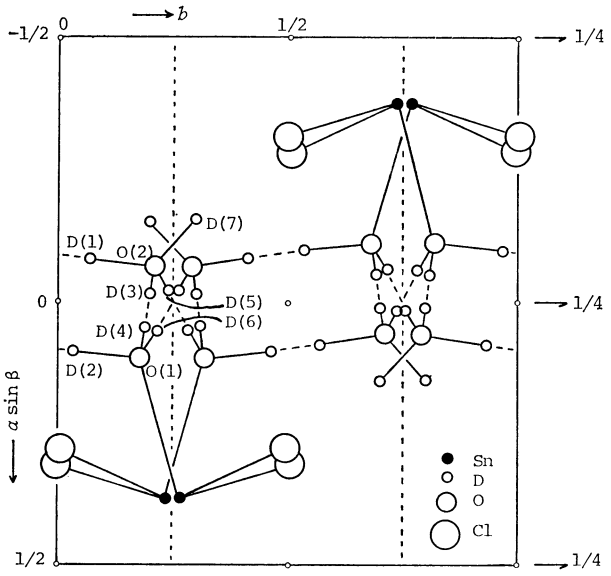

Fig. 1. The crystal sturcture projected on the (001) plane. The graphical symbols show the symmetry axes ($\bar{1}$ and 2_1) and the glide plane.

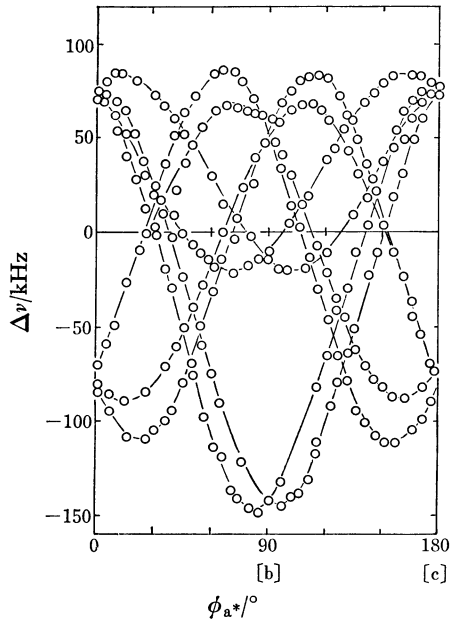

Fig. 2(a). The rotation pattern around the a* axis at 208 K.

potential for each H-bond, the seven sites shown in Fig. 1 are possible for four independent water–hydrogens.

Analytical Method. The quadrupole interaction in the present study can be treated as a first-order perturbation to the Zeeman energy, because the deuteron quadrupole coupling constant, e^2qQ/h, of about 200 kHz for a stationary water deuteron is much smaller than both Larmor frequencies of measurements. When a single crystal is turned about the z-axis, *i.e.*, for the z-axis rotation, the quadrupole splitting measured from the Larmor frequency, $\Delta\nu_z$, is expressed in the following convenient form:[12]

$$\Delta\nu_z = (3/8)(eQ/h)[V_{zz}^1-(V_{xx}^1-V_{yy}^1)\cos 2\phi-2V_{xy}^1\sin 2\phi] \quad (1)$$

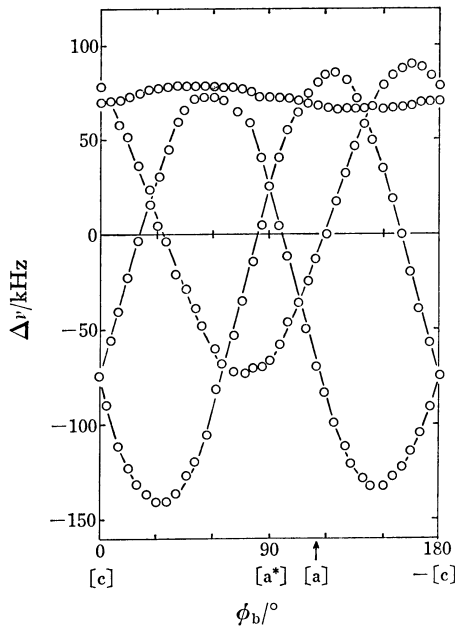

Fig. 2(b). The rotation pattern around the b axis at 208 K.

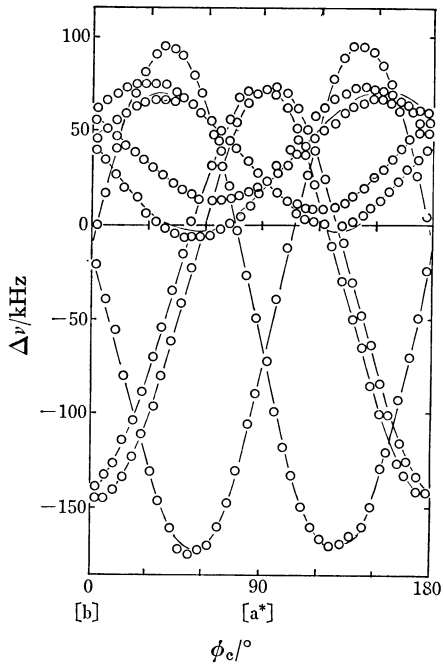

Fig. 2(c). The rotation pattern around the c axis at 208 K.

where V_{ij}^l is the electric-field gradient (EFG) tensor at a given deuteron site in the laboratory coordinate system (x, y, z) fixed to a probe head and where ϕ is the angle of the static magnetic field, H_0, measured from the reference axis (x-axis) on the rotation plane. The angular dependence or the rotation pattern of $\Delta\nu_z$ around the z-axis yields only the first three of the five independent EFG components, V_{xx}^l, V_{yy}^l, V_{xy}^l, V_{yz}^l, and V_{zx}^l. For this reason, the rotation patterns were measured around the three a*, b, and c axes, and then combined in the usual way. By diagonalizing the tensors thus obtained, the principal values and the direction cosines of the principal axes for every

Table 1. Quadrupole coupling constants(e^2qQ/h), asymmetry parameters(η), and direction cosines of the principal axes of the EFG tensors for Model I at 208 K, with the associated standard deviations in parentheses

	e^2qQ/h / kHz	η		Direction cosines a*	b	c
D (2)	194.2 (3)	0.066 (4)	q_{xx}	0.577 (24)	−0.141 (1)	−0.805 (17)
			q_{yy}	−0.815 (17)	−0.030 (4)	−0.579 (24)
			q_{zz}	−0.058 (1)	−0.990 (1)	0.132 (1)
D (4)	193.2 (5)	0.112 (3)	q_{xx}	−0.166 (13)	0.892 (6)	−0.420 (7)
			q_{yy}	0.843 (2)	0.349 (14)	0.409 (7)
			q_{zz}	−0.511 (1)	0.287 (1)	0.810 (1)
D (5)	223.3 (4)	0.206 (3)	q_{xx}	0.683 (4)	−0.721 (4)	−0.121 (3)
			q_{yy}	−0.552 (4)	−0.617 (4)	0.560 (1)
			q_{zz}	0.478 (1)	0.316 (1)	0.820 (1)
D (7)	244.0 (4)	0.058 (3)	q_{xx}	−0.205 (16)	−0.493 (17)	−0.846 (14)
			q_{yy}	−0.607 (6)	−0.614 (14)	0.505 (23)
			q_{zz}	−0.768 (1)	0.617 (1)	−0.173 (1)

Table 2. Quadrupole coupling constants, asymmetry parameters, and direction cosines of the principal axes of the EFG tensors for Model II at 208 K (standard deviations in parentheses)

	e^2qQ/h / kHz	η		Direction cosines a*	b	c
D (2)	194.2 (3)	0.066 (4)	q_{xx}	−0.577 (24)	−0.141 (1)	0.805 (17)
			q_{yy}	−0.815 (17)	0.030 (4)	−0.579 (24)
			q_{zz}	0.058 (1)	−0.990 (1)	−0.132 (1)
D (4)	195.0 (5)	0.066 (3)	q_{xx}	−0.455 (17)	−0.891 (1)	−0.005 (12)
			q_{yy}	−0.741 (10)	0.381 (20)	−0.553 (1)
			q_{zz}	−0.494 (1)	0.247 (1)	0.833 (1)
D (5)	223.0 (4)	0.117 (3)	q_{xx}	0.582 (7)	−0.813 (5)	−0.004 (6)
			q_{yy}	−0.647 (6)	−0.466 (9)	0.603 (1)
			q_{zz}	0.493 (1)	0.348 (1)	0.797 (1)
D (7)	244.0 (4)	0.058 (3)	q_{xx}	−0.205 (16)	−0.493 (17)	−0.846 (14)
			q_{yy}	−0.607 (6)	−0.614 (14)	0.505 (23)
			q_{zz}	−0.768 (1)	0.617 (1)	−0.173 (1)

EFG were determined in the crystallographic coordinate system.[13]

When a water molecule reorients rapidly at high temperatures, as in the present case, the EFG tensor for the moving deuteron should be averaged over the several sites spent by it. This averaging is actually performed by superposing the individual EFG's.

Results and Discussion

DMR Spectra in the Low-temperature Phase. Below the transition temperature (234 K), eight, four, and eight pairs of lines were observed about the a*, b, and c axes respectively, with a maximum splitting of about 180 kHz. These facts indicate that two non-equivalent water molecules are stationary in the low-temperature phase on the DMR scale. Every rotation pattern is consistent with the space group $P2_1/c$, which is the same as in the high-temperature phase. Thus, the present results provided no evidence in support of the antiferroelectric nature below T_t proposed by Mognaschi *et al.*,[7] in accord with the X-ray and ND results.

The rotation patterns measured at 208 K are presented in Fig. 2. As the figure shows, two independent pairs of sine curves cross at nearly the same point on each diagram when the magnetic field is along either the a*, b, or c axis. Therefore, the EFG tensors were calculated for 80 possible combinations of the sine curves. Such a large number of possibilities, however, was first reduced to one-half its initial number by assuming an e^2qQ/h value of about 200 kHz and an η value of nearly zero for a stationary water deuteron. Secondly, the number was further reduced to ten from the viewpoint of crystal symmetry involving the two-fold axis and the c-glide plane.

Then, we tried to assign the obtained EFG tensors to the individual deuterons on the basis of the following empirical rules:[12,14]

(1) the principal z axis of an EFG tensor is nearly

TABLE 3. RELATION BETWEEN THE DIRECTIONS OF THE PRINCIPAL AXES OF THE EFG TENSORS AT 208 K AND THE CONFIGURATION OF THE WATER MOLECULES IN SCD
(standard deviations in parentheses)

		O(1)		O(2)	
		D(2)	D(4)	D(5)	D(7)
ϕ_z/°	Model I	6.9(16)	11.2(15)	3.0(39)	—
	Model II	14.0(22)	9.2(19)	3.0(38)	—
	ND	6.1(33)	8.0(29)	2.3(34)	—
ψ_z/°	Model I	10.9(22)	4.1(26)	1.1(42)	1.1(34)
	Model II	8.3(24)	2.3(25)	1.4(44)	1.1(34)
θ_{yy}/°	Model I	20.9(31)		4.7(76)	
	Model II	20.7(35)		10.5(107)	
θ_{zz}/°	Model I	98.5(1)		108.3(1)	
	Model II	112.5(1)		107.6(1)	
	ND	104.0(5)		106.4(5)	

parallel to the direction of an O–D bond, and

(2) the principal y axis is nearly perpendicular to the molecular plane of D_2O.

The assignment based on the empirical rules successfully reduced the combination number to only two. For these models, I and II, the values of e^2qQ/h and η are summarized in Tables 1 and 2, where the direction cosines of each EFG principal axis are also included. In practice, however, no significant difference is observed between them in regard to the deuteron arrangement, *viz.*, the configuration of the water molecules of interest.

Configuration of Water Molecules. As has been described previously, the crystal structure suggests three and four available deuteron sites in the neighborhoods of O(1) and O(2) respectively.[2] If the Bernal and Fowler rules hold for the H-bonded water layers in SCD, then three of deuteron arrangements or of H-bonding schemes may be anticipated for an ordered state below T_t. Of these, only one type of scheme could be judged by the assignment of EFG for either model. The results obtained were in good agreement with the ND results, in turn supporting our assignment (Fig. 3a).

In Table 3, the configurations of water molecules for Models I and II are compared with those from the ND work, by using four characteristic angles, ϕ_z, ψ_z, θ_{yy}, and θ_{zz}; ϕ_z is the angle between the principal z-axis and the assigned O(D)···O direction of a deuteron; ψ_z, the angle between the principal z-axis and the O–D direction determined by ND; θ_{yy}, the angle between the principal y axes at two deuteron sites of a water molecule, and θ_{zz}, the corresponding angle between the two principal z axes.

The ϕ_z angle is widely spread, from 3° to 14°, and its maximum was found at $D_2O(1)$, probably because of its small acceptor angles, O···O(1)···O, such as 90.2° at 88 K (88.2° at 297 K).[4] On the other hand, the values of ψ_z are nearly zero, within the limit of experimental error, except for D(2). These facts provide additional evidence for the validity of the empirical rule (1) which has been used for suggesting O–D directions on the basis of the DMR results. The θ_{yy} values of $D_2O(1)$ in both models are about 21°,

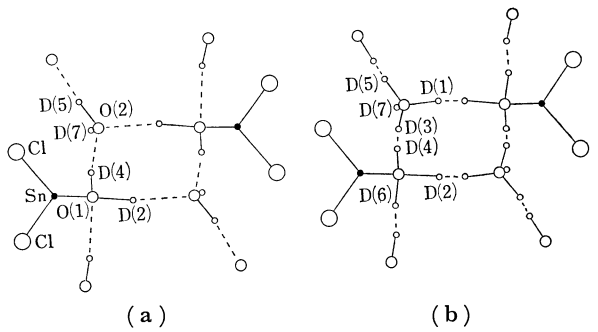

Fig. 3. Configuration of water molecules in (a) low- and (b) high-temperature phases.

considerably larger than the experimental values in the literature. The θ_{zz}'s of $D_2O(2)$ for both models are very close to the average bond-angle (108°) for water molecules of crystallization, and also to the ND results. Concerning the θ_{zz}'s of $D_2O(1)$, a slight but significant difference was disclosed between the two models. That is, the θ_{zz} values are 98.5° for the configuration Model I and 112.5° for II, compared with the D–O–D angle of 104.0° at 88 K (102.7° at 297 K) obtained from the ND results. In addition to the fact that the bond angle of a water molecule may be affected by forming O–D···O hydrogen bonds only a little, the EFG at the deuteron site may be influenced to some extent by the H-bonded-acceptor oxygen. It is, therefore, probable that the θ_{zz} of $D_2O(1)$ is smaller than the D–O(1)–D bond angle determined by ND; for this reason, Model I has been chosen as the basis for further discussion.

As has been mentioned earlier, Salinas and Nagle proposed a statistical model of the two-dimensional H-bonded network in SCD. They succeeded in predicting the temperature dependence of hydrogen occupancy at individual sites as well as the deuteron arrangements in the ordered structure.[10] On the other hand, Wang *et al.* demonstrated that the intensity of the Raman spectra associated with H-bonded vibrations changes gradually and continuously near T_t. They discussed this feature on the basis of the occupation probabilities of hydrogens at the various sites.[9] Under these circumstances, it became necessary to confirm whether or not the present DMR data are of the completely ordered state, because the temperature of the measurements, 208 K, is lower than T_t by only 26 K. However, the experimental results regarding the two-fold b-axis showed that the resonance line assignable to D(5) has almost the same intensity as those of the remaining three lines and that no absorption due to D(6) can be detected. It is, therefore, certain that the ordered arrangements of deuterium atoms are well established, even at 208 K, at least on the DMR scale. Unfortunately, no spectra could be observed below 200 K, possibly because of the very long spin-lattice relaxation times.

H-bonds in the Ordered-phase below T_t. It has been recognized that the quadrupole coupling constant of a deuteron, e^2qQ/h, reflects the H-bond strength and, consequently, depends on the O···O distance or, more precisely, on the D···O distance. Soda and

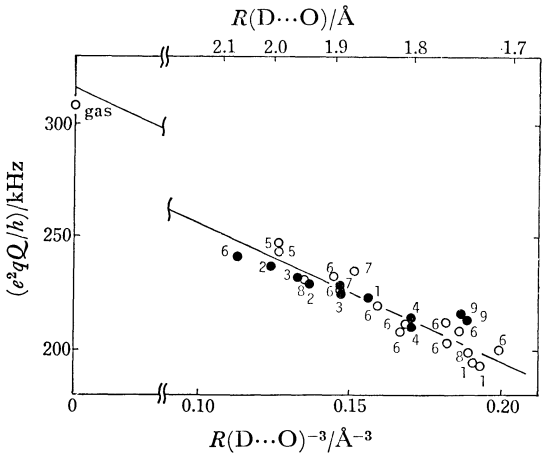

Fig. 4. Correlation between the observed quadrupole coupling constants and the reciprocal cube of hydrogen bond length R(D···O) in O-D···O type of hydrogen bonds. Black circles indicate the plot for non-coordinated water molecules. The plots correspond to 1: $SnCl_2 \cdot 2D_2O$ (this work and Ref. 4), 2: α-$(COOD)_2 \cdot 2D_2O$,[17,18] 3: β-$(COOD)_2 \cdot 2D_2O$,[17,18] 4: $(KCOO)_2 \cdot D_2O$,[19,20,21] 4: $Ba(ClO_3)_2 \cdot D_2O$,[12,22,23] 6: $CuSO_4 \cdot 5D_2O$,[15,24] 7: $NaHC_2O_4 \cdot D_2O$[25] 8: $LiHCOO \cdot D_2O$,[26,27] and 9: D_2O(Ice).[28,29]

Chiba first derived a useful relation based on the available DMR and ND results:[15]

$$e^2qQ/h = 310.0 - 3.0 \times \frac{190.6}{R(\mathrm{D}\cdots\mathrm{O})^3} \quad \text{(in kHz)}, \qquad (2)$$

where R(D···O) is the D···O distance in Å units. The coefficient, 190.6(kHz), is the e^2qQ/h value of a deuteron due to a unit charge placed apart from it by 1 Å. It is noteworthy that the constant, 310.0 kHz, is close to the e^2qQ/h value (307.95 kHz)[16] for a free water molecule in spite of the lesser reliablity of the early ND data. By using more reliable, three-dimensional ND results, including those in SCD, value of e^2qQ/h is plotted again as a function of R(D···O) in Fig. 4. The least-squares fitting on the 27 data points of nine hydrated crystals as well as of ice gave the following relation:

$$e^2qQ/h = 317.1 - 3.0 \times \frac{200.2}{R(\mathrm{D}\cdots\mathrm{O})^3} \quad \text{(in kHz)}, \qquad (3)$$

where, the coefficient, 200.2 kHz, is based on a recent, experimental value of eQ (2.875×10^{-27} cm²).[30] As can be seen in Fig. 4, no discrimination between coordinated water molecules and non-coordinated ones is necessary at all for relating e^2qQ/h to R(D···O). The above relationship will be used below to estimate the unknown value of e^2qQ/h from a known R(D···O).

DMR Spectra in the High-temperature Phase. The pair separation, $2\Delta\nu$, and the width of each component line were almost unchanged up to T_t (234 K), above which the whole spectra disappeared. As the temperature was further raised up to about 280 K, the signal again became observable. Figure 5 represents a typical temperature dependence of the quadrupole splitting at a rotation angle of $\phi_b = 95°$ around the two-fold b axis where the ϕ_b angle is measured away from the positive c axis toward the positive a axis

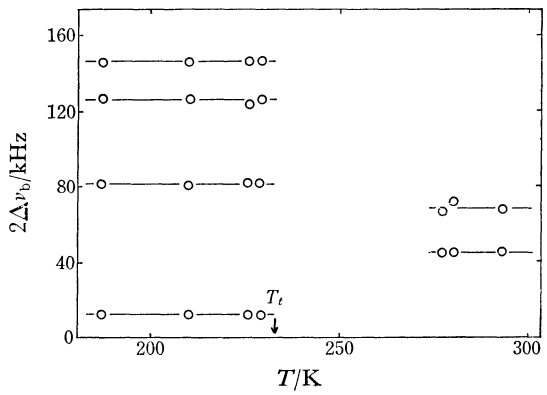

Fig. 5. The temperature dependence of quadrupole splittings around b-axis. $\phi_b = 95°$.

on the b plane (010). It should be noted that, in the high-temperature phase, the number of splitting is reduced by half and the pair separation, $2\Delta\nu$, decreases to less than half its low-temperature, rigid-lattice value. These facts indicate that all the deuterons are in some motional state above T_t and that their rate becomes fast enough to make the high-temperature spectra observable above 280 K. Since the S/N ratio of the signal was very poor, no motional parameter of deuterons could be estimated from the collapse of the splitting lines or line broadening. The above feature of the spectra, however, can be explained by assuming that the correlation time for deuterons is of the same order as for protons; the values determined from the pulsed PMR measurement are 2.3×10^{-5} and 2.3×10^{-7} s at 230 and 280 K respectively.[5]

Additionally, the high-temperature signal was observable only in a restricted angular region of less than 50° around the a* direction, which is perpendicular to the H-bonded water layer. The angular dependences of the experimental quadrupole splitting about the b and c axes are reproduced in Fig. 6.[5] The spectrum about the b axis clearly splitted into two pairs of lines. This finding, together with the symmetry relation, allowed us to expect the observation of four pairs of lines for the c-axis rotation. The outermost lines indeed showed the doublet structure at ϕ_c's of 105° and 110°, corroborating this expectation.

Deuteron Motion in the High-temperature Phase. The maximum splitting at room temperature is only about 40 kHz, much smaller than that expected for the two-fold reorientation, *i.e.*, the 180° flipping of water molecules. In the present case, however, the average EFG tensors for moving deuterons cannot be deduced because of the incomplete data above T_t. In order to clarify the dynamic process responsible for the deuteron disordered structure, we tried to simulate the rotation pattern for various types of motion suggested by the ND results (Fig. 3b). The average EFG for the moving deuteron in question was computed by using the method described previously. In this calculation, the empirical rules (1) and (2), and either the typical, found or expected values for e^2qQ/h and η in the stationary state were used. Then, the validity of each motional model was judged by the number of component lines about

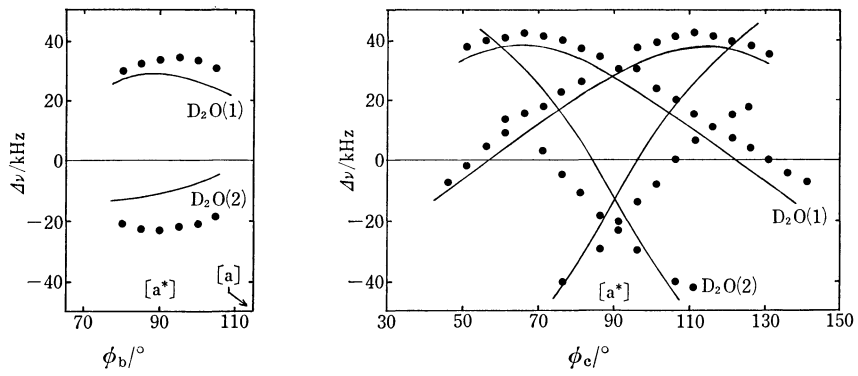

Fig. 6. Rotation patterns around (a) b-axis and (b) c-axis at room temperature. Soild curves indicate the calculated ones for Motion 5.

the unique b-axis, the width of quadrupole splitting, $\Delta\nu$, and its angular dependence.

First, the following three types of motion were checked:

Motion 1: *The 180°-flip of water molecules about each two-fold axis, as is found in many hydrated crystals.* The rotation pattern simulated about the b axis coincides with the observation in the number of splitting, but it differs greatly from the measurement in its magnitude and angular dependence.

Motion 2: *The jump motion of deuterons between two equilibrium positions in an O–D···O deuteriun bond, as is recognized in some H-bonded crystal like ferroelectric KH_2PO_4 substances.* This type of motion leads to four pairs of lines, which are assigned to the D(1)–D(2), D(3)–D(4), D(5)–D(6), and D(7) sites illustrated in Fig. 3b, in disagreement with the observation of only two pairs.

Motion 3: *The hindered rotation of both kinds of water molecules about their pseudo-three-fold axes, as proposed from the earlier ND results.*[5] In such a case, because one deuteron of $D_2O(2)$ is fixed at the D(7) site, three pairs of lines are expected; they are assigned to the D(7) and D(1)–D(3)–D(5) sites for $D_2O(2)$ and the D(2)–D(4)–D(6) sites for $D_2O(1)$, with an intensity-ratio of 1 : 1 : 2. This motion can also be excluded in view of the number of splitting.

Hence, it became necessary to combine either two or three of the above three types of motion in order to explain the experimental results. The following models were further examined:

Motion 4: *The combination of Motions 1 and 2.* This model gives rise to only a single spectral line, because all deuterons can move from one to another throughout all the seven deuteron sites, D(1)—D(7). Therefore, this can not be the case.

Motion 5: *The combination of Motions 1 and 3.* Two pairs of spectral lines are anticipated, because two deuterons of $D_2O(1)$ exchange their sites among the D(2), D(4), and D(6) sites, while those of $D_2O(2)$ do so among the D(1), D(3), D(5), and D(7) sites. The rotation pattern for this model was tentatively calculated by using the typical values of e^2qQ/h (=220 kHz) and $\eta(=0)$ for all the deuterons, regardless of the difference in H-bond strength discussed above. On averaging the EFG tensors, it must be taken into account that the molecular planes of both $D_2O(1)$ and $D_2O(2)$ change their orientations through Motion 5, with the probabilities depending on the occupancy factors of the individual deuteron sites, which are determined by the ND study. The occupancies of the D(2), D(4), and D(6) sites for $D_2O(1)$ were initially approximated by 2/3, while those of the D(1), D(3) and D(5) sites were approximated by 1/3 and that of D(7) by 1 for $D_2O(2)$.[3] Thus, the simulated rotation patterns around the b and c axes resemble to the experimental ones, especially in the magnitude of splitting and number (Fig. 3 in Ref. 5). This adequacy of the model led us to compute the rotation pattern based on the reasonable coupling constants derived from Eq. 3 and on the occupancies obtained from the ND study.[4] The results are shown in Fig. 6. The fit to the observation is not very good, but the agreement between them seems satisfactory enough in view of the oversimplified model and the uncertainty in both DMR and ND experiments at room temperature.

Motion 6: *The combination of Motions 2 and 3.* Two pairs of lines with the intensity ratio of 1 : 3 are to be expected for the b-axis rotation; the former is assigned to the D(7) site, and the latter, to all the other sites from D(1) to D(6). Since the observed intensity ratio was almost 1 : 1, this model is not adequate.

Motion 7: *The combination of Motions 1, 2, and 3.* Because all deuterons can travel to all the deuteron sites, from D(1) to D(7), the b-rotation pattern may be expected to consist of only one pair of lines, in conflict with the observation.

It is, therefore, concluded that the motion of deuterium atoms in the high-temperature, disordered phase of SCD is best described as a combination of the 180°-flip and the hindered rotation about the Sn–O(1) and D(7)–O(2) bonds for $D_2O(1)$ and $D_2O(2)$ respectively. The direction of Sn–O(1) makes an angle of 16° with the axis normal to the H-bonded water layer, *viz.*, the a* axis, while the corresponding angle for D(7)–O(2) amounts to 41°.

The proton dynamics associated with the phase transition, as has been mentioned previously, have been investigated by Mognaschi *et al.*[7] They explained the critical phenomena of the dielectric constant in terms of a "critical slowing down" of the electric polarization, which was ascribed to the proton

transfer along an H-bond in a double-minimum potential. We cannot discuss such critical behavior from the viewpoint of DMR, since our data are lacking in the vicinity of T_t. On the other hand, a logarithmic plot of the proton spin-lattice relaxation times *vs.* the reciprocal temperature showed a deep, cusp-shaped reduction around T_t, in contrast to the prediction by Mognaschi *et al.*[5,7] The structural information from X-ray results may be significant in this regard. On passing through the transition, the distances of the three non-equivalent H-bonds vary with the temperature in different ways. Consequently, the resulting change in the potential energy makes the critical dynamics too complex to discuss in the light of the present theories.

The present DMR study has shown that the dynamic process occuring in the high-temperature phase well above T_t is assignable to Motion 5, that is, the combination of the 180°-flip and pseudo-C_3 reorientation of water molecules, excluding the deuteron transfer. Therefore, even if the jump motion along an H-bond is involved in the disordered phase, its rate must be too slow to affect the DMR spectra. In the earlier paper we pointed out that the noticeable d.c. conductivity found in SCD is attributable to the proton mobility, as with ice.[1] Mognaschi *et al.* have recently provided strong evidence for the protonic conduction and proposed a combination of the translation of protons along H-bonds and the rotation of water molecules as the conduction mechanism.[31] Another striking feature of our model is that the deuteron at D(7), whcih is free from any deuterium-bond, is not stationary, but travels among the four allowed sites around D(2). The occupancy factor at D(7) is expected to be unity, the same as in the low-temperature, ordered state, this being consistent with the ND results.

The authors wish to express their thanks to Professor Emeritus Ryôiti Kiriyama of Osaka University for his continued interest and fruitful discussion.

References

1) H. Kiriyama and R. Kiriyama, *J. Phys. Soc. Jpn.*, **28**, S114 (1970).
2) H. Kiriyama, K. Kitahama, O. Nakamura, and R. Kiriyama, *Bull. Chem. Soc. Jpn.*, **46**, 1389 (1973).
3) R. Kiriyama, H. Kiriyama, K. Kitahama, and O. Nakamura, *Chem. Lett.*, **1973**, 1105.
4) K. Kitahama and H. Kiriyama, *Bull. Chem. Soc. Jpn.*, **50**, 3167 (1977).
5) H. Kiriyama, O. Nakamura, and R. Kiriyama, *Chem. Lett.*, **1976**, 689.
6) T. Matsuo, M. Tatsumi, H. Suga, and S. Seki, *Solid State Commun.*, **13**, 1829 (1973); T. Matsuo, M. Oguni, H. Suga, and S. Seki, *Bull. Chem. Soc. Jpn.*, **47**, 57 (1974).
7) E. R. Mognaschi, A. Rigamonti, and L. Menafra, *Phys. Rev. B*, **14**, 2005 (1976).
8) H. Morisaki, H. Kiriyama, and R. Kiriyama, *Chem. Lett.*, **1973**, 1061.
9) C. H. Wang, M. Tatsumi, T. Matsuo, and H. Suga, *J. Chem. Phys.*, **67**, 3097 (1977).
10) S. R. Salinas and J. F. Nagle, *Phys. Rev. B*, **9**, 4920 (1974). S. R. Salinas and J. F. Nagle, *J. Phys. Soc. Jpn.*, **41**, 1643 (1976).
11) H. Kiriyama, O. Nakamura, and R. Kiriyama, *Acta Crystallogr., Sect. A*, **28**, S240 (1972).
12) T. Chiba, *J. Chem. Phys.*, **39**, 947 (1963).
13) G. M. Volkoff, H. E. Petch, and D. W. L. Smellie, *Can. J. Phys.*, **30**, 270 (1952).
14) R. Bersohn, *J. Chem. Phys.*, **32**, 85 (1960).
15) G. Soda and T. Chiba, *J. Chem. Phys.*, **50**, 439 (1969).
16) J. Verhoeven, A. Dymanus, and H. Bluyssen, *J. Chem. Phys.*, **50**, 3330 (1969).
17) T. Chiba and G. Soda, *Bull. Chem. Soc. Jpn.*, **44**, 1703 (1971).
18) P. Coppens and T. M. Sabine, *Acta Crystallogr., Sect. B*, **25**, 2442 (1969).
19) B. Pedersen, *Acta Chem. Scand.*, **22**, 453 (1968).
20) J. W. McGrath and G. W. Ossman, *J. Chem. Phys.*, **46**, 1824 (1967).
21) A. Sequeira, S. Srikanta, and R. Chidambaram, *Acta Crystallogr., Sect. B*, **26**, 77 (1970).
22) K. Haland and B. Pedersen, Proc. Colloq. Amp. 15th, Amsterdam (1969), p. 409.
23) S. K. Sikka, S. N. Momin, H. Rajagopal, and R. Chidambaram, *J. Chem. Phys.*, **48**, 1883 (1968).
24) G. E. Bacon and D. H. Titterton, *Z. Krystallogr.*, **141**, 330 (1975).
25) B. Berglund and J. Tegenfeldt, *Mol. Phys.*, **26**, 633 (1973).
26) B. Berglund, J. Lindgren, and J. Tegenfeldt, *J. Mol. Struct.*, **21**, 135 (1974).
27) R. Tellgren, P. S. Ramanujam, and R. Liminga, *Ferroelectrics*, **6**, 191 (1974).
28) P. Waldstein, S. W. Rabideau, and J. A. Jackson, *J. Chem. Phys.*, **41**, 3407 (1964).
29) S. W. Peterson and H. A. Levy, *Acta Crystallogr.*, **10**, 70 (1957).
30) R. V. Reid, Jr., and M. L. Vaida, *Phys. Rev. Lett.*, **29**, 494 (1972).
31) E. R. Mognaschi, A. Chierico, and G. Parravicini, *J. Chem. Soc., Faraday Trans. 1*, **74**, 2333 (1978).